Supramolecular chain-like aggregates and polymeric sandwich complexes constructed from *p*-sulfonatocalix[4,6]arenes with (8-hydroxy)quinoline guests†‡

Yu Liu,* Qiang Li, Dong-Sheng Guo and Kun Chen

Received 19th November 2007, Accepted 3rd January 2008
First published as an Advance Article on the web 7th February 2008
DOI: 10.1039/b717884k

Three crystalline complexes were prepared by the inclusion complexation of *p*-sulfonatocalix[4]arene with quinoline (**1**), *p*-sulfonatocalix[6]arene with quinoline (**3**) and 8-hydroxyquinoline (**4**), respectively. These crystals were compared to the reported *p*-sulfonatocalix[4]arene complex with 8-hydroxyquinoline (**2**). The results obtained show that *p*-sulfonatocalix[4]arene forms 1 : 1 included complexes for (8-hydroxy)quinoline guests with the pinched-cone conformation, whereas *p*-sulfonatocalix[6]arene forms 1 : 2 complexes with the centrosymmetric 'up–down' double partial cone conformation. Furthermore, the aggregation structures of complexes **1**–**4** are diverse from the common bilayer array for **2** to the chain-like aggregation for **1** and to the polymeric sandwich complexes for **3** and **4**. These observations are carefully discussed from the viewpoints of host conformation, host–guest binding structure and stoichiometry, and the effect of counterion.

Introduction

Crystal engineering is a focus area for constructing a number of interesting network structures with some special tectons. In the system of supramolecular chemistry, the host and guest components may have the opportunity to construct various spectacular extended structures in the solid state through noncovalent interactions between the molecular subunits, such as coordination, electrostatic, hydrogen-bonding, and π-stacking interactions. As one kind of versatile building blocks, *p*-sulfonatocalix[*n*]arenes (CnAS) have played a substantial role in this field. CnAS, possessing various characteristics of multicharge, flexible cavity and amphipathic properties,[1] can interact with a range of guest species with different size/shape, including organic, charged organic, inorganic molecules or ions.[2] Upon complexation with different guest molecules, they can construct many other splendid supramolecular architectures besides the general bilayers,[3] such as 'molecular capsules',[4] 'ferris wheel',[5] 'Russian doll',[6] spheres and tubular arrays,[7] coordination polymers,[8] and 2-D hydrogen polymers,[9] *etc.* In fact, the smallest analogue, C4AS, has been widely engaged in this field and a series of achievements have been gained[10] due to its ease of synthesis, rigid conformation, complex crystallization and less problematic in collection and refinement of single-crystal diffraction data.[4] Recently, C6AS, the larger analogue, has also gained comparative attention in constructing kinds of solid-state aggregation. In comparison with C4AS, C6AS possesses some intrinsic characteristics of higher charge, more flexible framework and a bigger cavity size. Particularly, C6AS are dramatically pronounced to be a di-topic receptor with 'up–down' or 'up–up' conformations. As a result, despite a few disadvantages of material refinement and complex crystallisation, C6AS promises to be a big-potential building block for constructing more spectacular supramolecular architectures. As reported by Atwood and Raston *et al.*, C6AS can also assemble into the bilayer array with either 'up–down' double partial cone[11] or 'up–up' double cone[12] conformations. For example, in the presence of pyridine *N*-oxide/nickel(II) or 4,4′-dipyridine-*N,N*′-dioxide/europium(III), C6AS forms the typical bilayer arrangement in 'up–down' double partial cone conformation, whereas upon complexation with pyridine *N*-oxide/lanthanum(III), C6AS forms the corrugated bilayer arrangement within the extended structure.[11] More interestingly, the bilayer structure of C6AS can be destroyed once the pyridine *N*-oxide/ytterbium(III) guest has been employed. And the C6AS tectons in the complex assemble themselves into sheet-like arrangements through the intricate hydrogen bondings.[13] In addition, based on the 'up–up' double cone conformation, C6AS can present the double 'molecular capsule' arrangement shrouding two 18-crown-6/terbium(III) while the 'ferris-wheel' arrangement in the presence of 18-crown-6/europium(III).[14] C6AS can also astrict two tetraphenylphosphonium guests to form a molecular capsule-like arrangement.[15] More recently, we also reported novel polymeric capsules and honeycomb aggregates formed by C6AS with phenanthrolinium compounds.[16]

Although there have been several reports on the supramolecular architectures constructed by C4AS and C6AS upon complexation with the same guests,[7,11–16,17] a close comparison between the inclusion and aggregation structures between C4AS and C6AS in the presence of the same guests has been concerned less frequently. On further pursuing the supramolecular architectures based on CnAS, we wish to report herein on the structures of three solid-state complexes, including C4AS with quinoline (QU) (**1**), C6AS with QU (**3**) and

Department of Chemistry, State Key Laboratory of Elemento-Organic Chemistry, Nankai University, Tianjin, 300071, P. R. China. E-mail: yuliu@nankai.edu.cn; Fax: +86-22-23503625; Tel: +86-22-23503625

† CCDC reference numbers 657145–666758. For crystallographic data in CIF or other electronic format see DOI: 10.1039/b717884k

‡ Electronic supplementary information (ESI) available: Structures of the complexes studied (Fig. S1–S4). See DOI: 10.1039/b717884k

8-hydroxyquinoline (8-HQ) (**4**). The obtained results are discussed carefully from the viewpoints of the host–guest binding stoichiometry, binding geometry and a further extended structure together with the complex of C4AS with 8-HQ (**2**) reported before.[18]

Results and discussions

All complexes are synthesized by reacting the corresponding CnAS and (8-hydroxy)quinoline guests at room temperature in acidic solution (see Experimental section). Complexes **1**–**4** crystallize in a monoclinic space group $P2_1/c$, triclinic space group $P\bar{1}$, triclinic space group $P\bar{1}$ and triclinic space group $P\bar{1}$, respectively. Their asymmetric units contain the following: 1 crystallographically distinct C4AS, 3 protonated quinoline guests (QU^+) and 9 water molecules for **1**; 1 C4AS, 3.5 protonated 8-hydroxyquinoline guests ($8\text{-}HQ^+$) and 13.5 water molecules for **2**; 0.5 C6AS, 3 QU^+ and 9.25 water molecules for **3**; 0.5 C6AS, 3 $8\text{-}HQ^+$ and 10.5 water molecules for **4**. Among these crystals, some sulfonate groups of CnAS, the guest molecules and several water molecules are disordered at two or more positions, respectively. The results of the conformations of CnAS, host–guest binding geometries and the extended structures of the complexes will now be discussed in detail.

Crystal structures

$[C4AS^{4-}+H^+][QU^+]_3\cdot 9\ H_2O$ (1). As shown in Fig. 1a, in complex **1**, the QU guest is included slantways into the cavity of C4AS with part of the pyridine ring immersed. Different types of noncovalent interactions between C4AS and QU are observed, including two C–H···π interactions (C–H···centroid of an aromatic ring: 2.579(1) Å, 159.72(1)°; 2.574(1) Å, 162.76(1)°) and two unconventional hydrogen bonds (C–H···O: 2.42(1) Å, 174.72(2)°; N–H···O: 3.62(1) Å, 139.99(2)°). The ^{1}La axis of QU forms an angle of 27.1° with the plane defined by four bridging methylenes.[19] To accommodate well the planer aromatic QU guest, C4AS adopts the pinched-cone conformation (C_{2v} symmetry), which is elucidated by the S···S distances between the opposite sulfonate groups [12.122(1) Å and 8.843(11) Å, respectively]. Therefore, the actual ϕ and χ torsion angle values, which are used to define the solid state conformation of C4AS according to the Ugozzoli–Andreetti convention,[20] are +86.93(2), −107.86(1); +98.39(1), −72.45(2); +83.69(2), −107.09(1); +99.93(1), −75.00(2). In comparison with complex **2** of C4AS with 8-HQ, their host conformations and host–guest including geometries are similar to each other. In complex **2**, C4AS also adopts the C_{2v} cone conformation [S···S approaches of *trans* sulfonates: 11.7822(33) Å, 8.3423(19) Å; the actual ϕ and χ torsion angle values: +75.37(2), −97.45(2); +95.32(2), −79.64(2); +81.58(2), −104.07(2); +102.76(2), −75.18(2)] with the pyridine portion of 8-HQ immersed into the cavity (the angle formed by the ^{1}La axis of 8-HQ and the plane defined by four bridging methylenes: 42.5°) (Fig. 1b).

However, the extended structures between complexes **1** and **2** differ a lot from each other. In complex **2**, each C4AS molecule is surrounded by three other C4AS molecules and one 8-HQ counterion through four π···π interactions, which presents the common bilayer arrangement. However, close examination of the extended structure of complex **1** found that there are none of the π-stacking interactions between calixarenes (the main driving forces to construct the bilayer array) detected. As a result, the aggregate of C4AS in complex **1** presents the chain-like structure extending along the calixarene cavity axis, which noticeably deviates from the conventional bilayer array. As shown in Fig. 2a, the C4AS molecules link head-to-tail through the hydrogen bonds between the phenolic hydroxyls and sulfonate groups [O–H···O: 2.679(2) Å, 144.97(2)°] to form an infinite prolonging chain-like structure along the crystallographic *c* axis. Each chain runs in the opposite direction to the adjacent ones, which are further linked together through dual unconventional hydrogen bonds [C–H···O: 3.457(4) Å, 163.64(1)°] to form an interlocked net-like structure in the crystallographic $b \times c$ plane. Moreover, there is one disordered QU counterion filled in the interspace of the net to join the adjacent pillars together through π···π interactions (Fig. 2b). Viewed from the crystallographic *c* axis, the

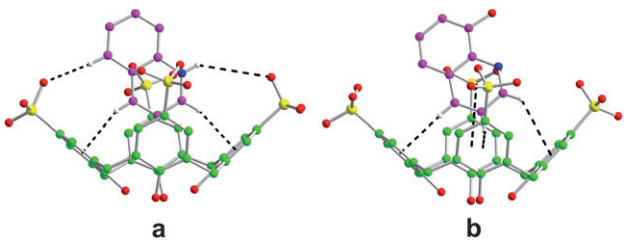

Fig. 1 View of the 1 : 1 complexes formed by C4AS: (a) for complex **1** and (b) for complex **2**. The dashed lines represent the noncovalent weak interactions including C–H···π and hydrogen bond interactions.

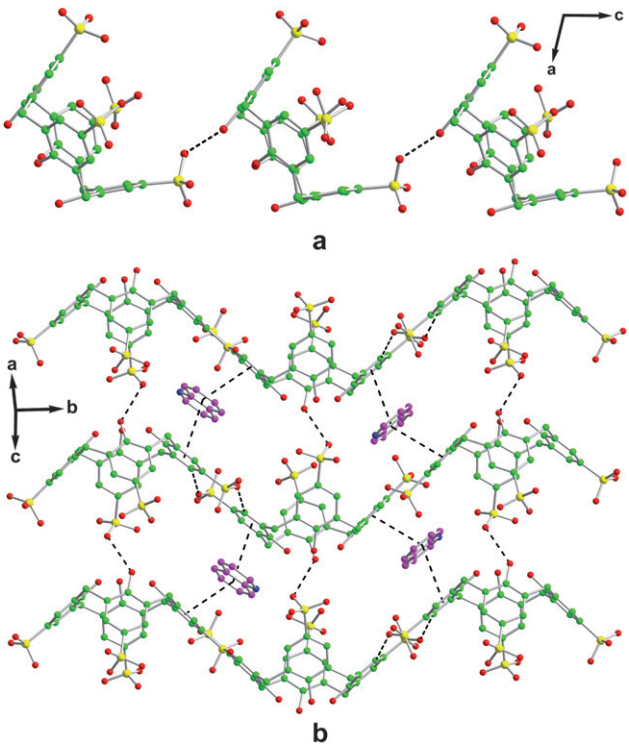

Fig. 2 View of the chain in complex **1** formed by C4AS molecules (a) and the net-like structure where the chains run in opposite directions are linked together by hydrogen bonds (b).

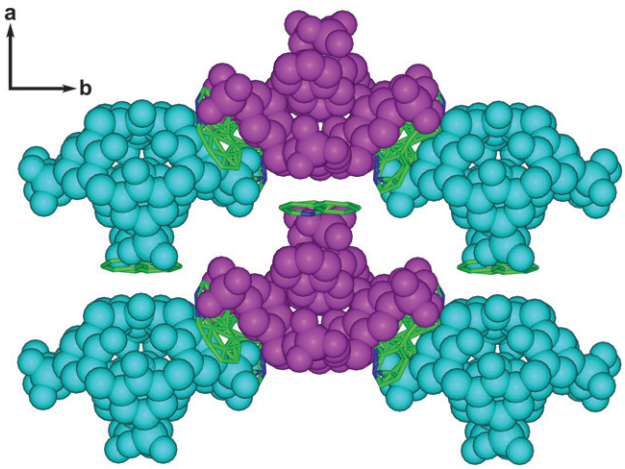

Fig. 3 View of the overall extended structure of complex **1**. These chains run perpendicular to the plane of the page and the ones extended in the same direction are shown in the same color.

overall structure of complex **1** also presents some characteristics of a layer array, in which each net-like structure on the crystallographic $b \times c$ plane represents one layer, and the other QU counterions are located between the layers (Fig. 3). However, the typical bilayer array of C4AS is completely abandoned in complex **1** as: (1) the dominating forces to construct the bilayer array are not observed; (2) one cannot find specifically the hydrophilic and hydrophobic layers.

[C6AS^{6-}][QU^{+}]$_6$·18.5 H$_2$O (3). In complex **3**, C6AS adopts a centrosymmetric 'up–down' double partial cone conformation where the actual ϕ and χ torsion angle values are −86.02(3), +105.13(3); −76.95(3), +99.43(3); +106.53(3), +13.26(4); −86.02(3), +105.13(3); −76.95(3), +99.43(3); +106.53(3), +13.26(4)°. So, one C6AS molecule contains two identical binding sites for QU guests, which leads to a 1 : 2 host–guest inclusion stoichiometry. As shown in Fig. 4a, two QU guests are simultaneously immersed into the 'up' and 'down' cavities of C6AS in which both portions of the phenyl and pyridine rings are included, differing from that in complex **1**. There are three independent host–guest noncovalent interactions donated by the aromatic rings of C6AS, including two C–H···π interactions between two carbon atoms of the QU guest and the neighboring aromatic rings of C6AS [C–H···centroid of the aromatic ring: 2.759(26) Å, 152.64(3)°; 2.637(24) Å, 151.45(3)°] and one π···π interaction [centroid of aromatic···centroid of aromatic: 3.571(36) Å]. In addition, the hydrogen atoms of the methylene bridges between 'up' and 'down' cavities point to the inner cavity, and then form a particular C–H···π interaction with the aromatic ring of QU [C–H···centroid of the aromatic ring: 2.633(25) Å, 125.65(2)°], which also reinforces the host–guest inclusion complexation. Besides the two included QU guests, each C6AS molecule is surrounded by four QU counterions to satisfy the charge balance, which also form π-stacking or hydrogen-bonding interactions with the exo-walls and sulfonate groups of C6AS [C–H···π interaction: C–H···centroid of aromatic ring: 3.423(18) Å, 103.82(2)°; π···π interaction: centroid of aromatic···centroid of aromatic: 3.615(28) Å; hydrogen bond: N–H···O: 2.832(25) Å, 128.08(3)°] (Fig. 4b).

Further, with regard to this structure, each included QU guest interacts with the other one in the adjacent unit through π···π interactions [centroid of aromatic···centroid of aromatic: 3.776(32) Å] to form a face-to-face QU-dimer (Fig. 5a). Therefore, the 2 : 1 sandwich complex is built by one QU-dimer and two face-to-face half-C6AS with a height of 11.064(1) Å (Fig. 5b). During sandwich formation, aside from the interactions between C6AS and QU, the stability of the sandwich complex is also reinforced by some noncovalent interactions from the water molecules. It can be seen from Fig. S1a that a total of 10 hydrogen bonds participate in closing the sandwich unit.‡ These hydrogen bonds are generated by two equivalent sets of three water molecules observed in the crystal structure. Each set of water molecules has five crystallographically distinct hydrogen bonds. For example, one set labelled O13, O14 and O16 has the following hydrogen-bond distance: O13···O1: 2.521(23) Å; O13···O14: 2.705(5) Å; O14···O16: 2.822(25) Å;

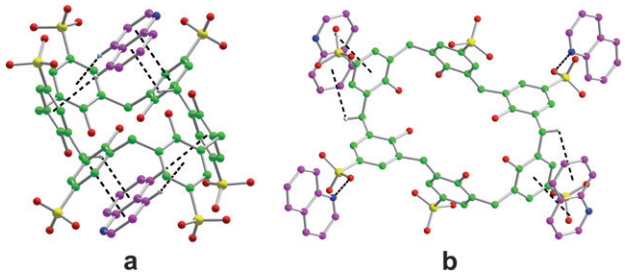

Fig. 4 View of the 1 : 2 complex formed by C6AS with QU (a) and the interactional mode of the C6AS with the four QU counterions around it (b) in complex **3**.

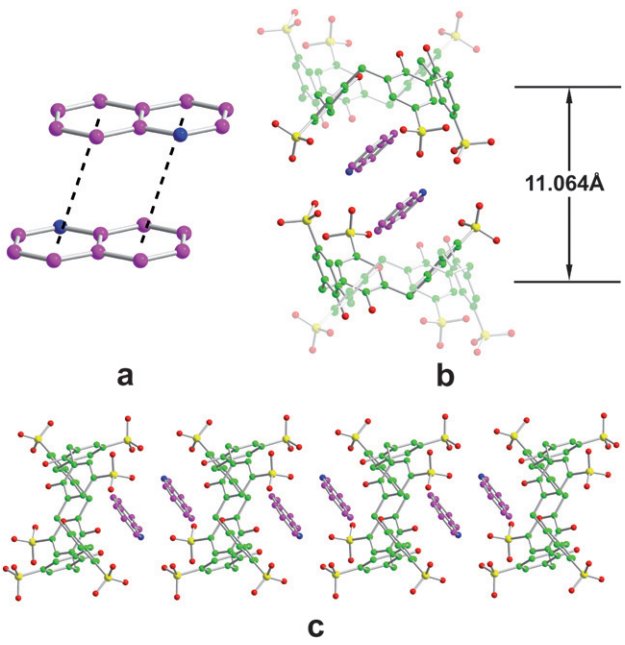

Fig. 5 View of the QU dimer (a), the sandwich unit formed by the two half-C6AS (shown in opaque) and one dimer (b) and the structure of the polymeric sandwich complexes along the crystallographic *a* direction in complex **3**.

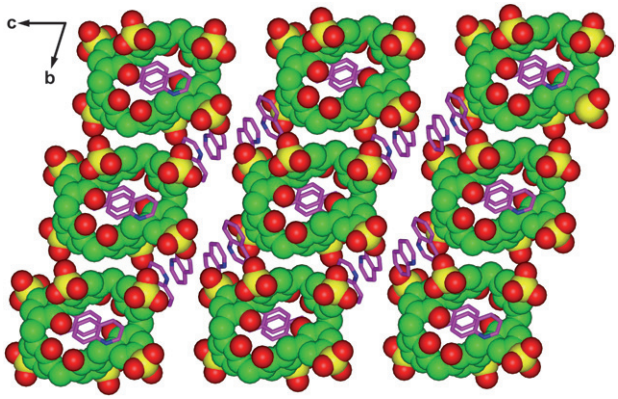

Fig. 6 View of the multipillar aggregate of complex **3** in the crystallographic $b \times c$ plane (polymeric sandwich complexes running perpendicular to the plane of the page), showing the QU molecules as counterions (in stick mode), which make the polymeric sandwich complexes isolated.

O13···O16: 2.664(19) Å; O16···O7: 2.783(35) Å. The sandwich unit extends infinitely along the crystallographic *a* direction to form polymeric sandwich complexes through the linkage of the covalent bonds between the 'up' cavity and the 'down' cavity of C6AS, which resemble the case of C6AS-Phen as reported before (Fig. 5c). At first glance the overall structure of complex **3** also presents a spacious layered structure character (see Fig. S2 in the ESI),‡ but scrutiny of the crystal packing reveals that there is none of the π-stacking or hydrogen-bonding interactions detected among calixarenes themselves to form the traditional bilayer array.[3,11,12] In other words, the bilayer extended structure of C6AS is broken up, and each C6AS molecule is separated by QU counterions. Hence, the extended structure of complex **3** presents the miltipillar aggregation, in which each set of polymeric sandwich complexes represents a pillar (Fig. 6). The QU counterions are located in the interspace among pillars, forming π-stacking and hydrogen-bonding interactions, as mentioned above.

[C6AS^{6-}][8-HQ^{+}]$_6$·21H$_2$O (4). C6AS also forms the host–guest 1 : 2 stoichiometry complex to 8-HQ with an 'up–down' double partial cone conformation [the actual ϕ and χ torsion angle values are +92.08(2), −27.58(3); +92.00(2), −75.66(2); +14.09(3), +115.64(2); +92.08(2), −27.58(3); +92.00(2), −75.66(2); +14.09(3), +115.64(2)°] in complex **4**. However, differing from the case of C4AS (**1** and **2**), C6AS provides two different binding geometries upon complexation with QU and 8-HQ guests. Although both the phenyl and pyridine rings of 8-HQ are also immersed into the cavity of C6AS, there are obvious differences on the orientations between QU in **3** and 8-HQ in **4**. As shown in Fig. 4a and 7a, the N atom of the QU guest points to the upper rim of C6AS, whereas that of the 8-HQ guest points to the lower rim of C6AS. There are two independent C–H···π interactions between two carbon atoms of the 8-HQ guest and the adjacent aromatic rings of C6AS [C–H···centroid of aromatic ring: 3.121(3) Å, 144.93(2)°; 3.807(8) Å, 137.78(2)°] and one C–H···π interaction between the carbon atom of the methylene in C6AS and the aromatic ring of the 8-HQ molecule [C–H···centroid of aromatic ring: 2.772(4) Å, 137.29(2)°] (Fig. 7a).

Complex **4** presents the structure of polymeric sandwich complexes in the same way (Fig. 7c), in which one 8-HQ-dimer and

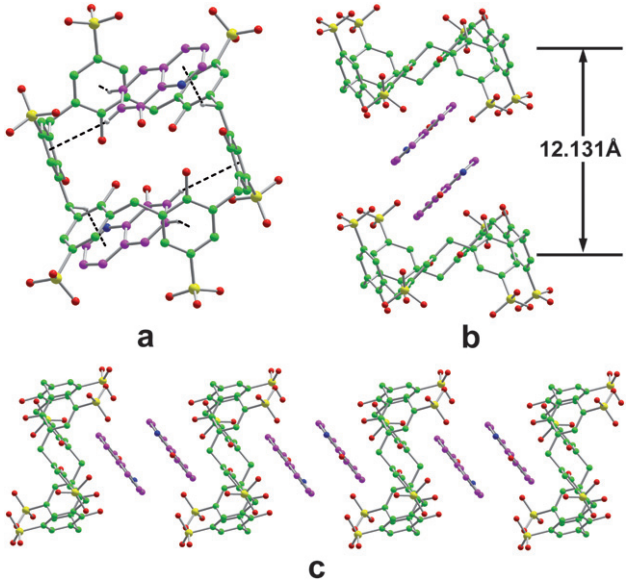

Fig. 7 View of the 1 : 2 complex formed by C6AS with 8-HQ (a), the sandwich unit formed by C6AS and 8-HQ dimer (b) and the structure of the polymeric sandwich complexes (c) in complex **4**.

two face-to-face half-C6AS compose the asymmetric sandwich unit with a height of 12.131(2) Å (Fig. 7b). There are also two equivalent sets of five water molecules located in the crystal structure to offer a total of 14 hydrogen bonds to reinforce the sandwich complex. One set labelled O16 to O20 has the following hydrogen-bond distance: O16···O8: 2.796(3) Å; O16···O20: 2.783(2) Å; O3···O20: 2.698(2) Å; O17···O4: 2.775(5) Å; O18···O17: 2.716(5) Å; O18···O19: 2.770(3) Å; O19···O12: 2.791(3) Å (see Fig. S1b in the ESI).‡ A notable comparison between complexes **3** and **4** should be concerned with the sandwich compactness. It can be seen from the given height values that the sandwich unit in complex **3** is more compact than that in complex **4**. The reason lies mainly in the orientation of the guest dimer in the cavity. In complex **3**, the dihedral angle is about 41.66°, which was formed by the plane of QU and the plane was defined by the three sulfur atoms (see Fig. S4 in the ESI),‡ whereas the corresponding angle in complex **4** is 50.22°. It means that the QU dimer is accommodated into the cavity in a more slantwise manner than the 8-HQ dimer, leading to better compactness of the sandwich unit in complex **3**. Moreover, the QU dimer forms additional dual hydrogen bonds with C6AS [N–H···O: 2.758(23) Å, 170.28(4)°], which also reinforces the sandwich compactness to some extent.

In spite of the similar structures of the polymeric sandwich complexes in complexes **3** and **4**, their overall aggregations differ from each other. Each C6AS host is surrounded by four 8-HQ counterions and two other C6AS molecules in complex **4** (Fig. 8a). Therefore, the calixarenes themselves arrange in chains rather than the typical bilayer array through π···π interactions [centroid of aromatic···centroid of aromatic: 3.912(6) Å] and hydrogen bonds [O–H···O: 2.784(5) Å, 163.28(3)°], in which each chain runs in the vertical direction of the calixarene cavity axis. When all the host and guest molecules are taken into account, complex **4** also presents an extended structure of multipillar aggregation (Fig. 8b), although with some residue

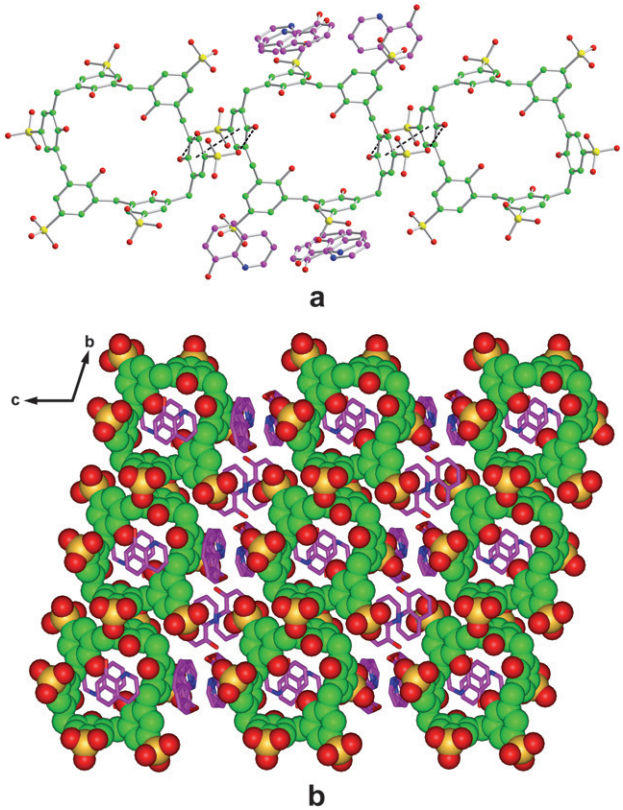

Fig. 8 View of the host molecule environment in a hydrophobic layer (a) and the multipillar aggregate of complex **4** in the crystallographic $b \times c$ plane (polymeric sandwich complexes running perpendicular to the plane of the page) (b).

of bilayer characteristics (see Fig. S3 in the ESI).‡ Differing from that in **3**, the pillars are directly joint together along the crystallographic *b* direction through the noncovalent interactions between calixarenes. In the crystallographic *c* direction, the pillars are separated by 8-HQ counterions.

Conclusions

Combining the present results and those reported before, it can be found that, upon complexation with QU guests, C4AS assumes a C_{2v} cone conformation with 1 : 1 binding stoichiometry, while C6AS assumes a centrosymmetric 'up–down' double partial cone conformation with 1 : 2 binding stoichiometry. In complexes **1** and **2**, only the portion of the pyridine ring of the guest is immersed in the cavity of C4AS; in complexes **3** and **4**, the pyridine and phenyl rings of the guest are simultaneously immersed in the cavity of C6AS with the phenyl ring prior to the pyridine ring. On careful comparison of the packing structures of complexes **1**–**4**, it is noticeable that the extended structures of C4AS complexes **1** and **2** differ from each other in the presence of the QU or 8-HQ guest—the common bilayer array for complex **1**, and the chain-like aggregation for complex **2**. However, both C6AS complexes **3** and **4** present the extended structures of polymeric sandwich complexes, in which there is some difference on the sandwich compactness between them.

Experimental

Materials

p-Sulfonatocalix[4, 6]arene were synthsised and purified according to a literature method, respectively.[21] Guest molecules, quinoline and 8-hydroxyquinoline, were commercially available and used without further purification.

Preparation of compounds

$[C4AS^{4-}+H^+][QU^+]_3 \cdot 9\ H_2O$ (1). To an aqueous solution of C4AS (50 mg, 20 mL), 4 equiv. of QU were added. Under stirring, 2 M HCl was added dropwise to adjust pH to 1∼2. Followed by filtration, the filtrate was placed for evaporation for about 2 weeks. Then the colorless crystal formed was collected along with its mother liquor for X-ray crystallographic analysis. Yield: 39% (30 mg, 0.023 mmol).

$[C6AS^{6-}][QU^+]_6 \cdot 18.5\ H_2O$ (3). To an aqueous solution of C6AS (50 mg, 20 mL), 6 equiv. of QU were added. Under stirring, 2 M HCl was added dropwise to adjust pH to 1∼2. Followed by filtration, the filtrate was placed to evaporation for about 3∼4 days. Then the colorless crystal formed was collected along with its mother liquor for X-ray crystallographic analysis. Yield: 42% (37 mg, 0.016 mmol).

$[C6AS^{6-}][8\text{-}HQ^+]_6 \cdot 21\ H_2O$ (4). To an aqueous solution of C6AS (50 mg, 20 mL), 6 equiv. of QU were added. Under stirring, 2 M HCl was added dropwise to adjust pH to 1∼2 and yellow dusty deposit appeared after several hours. Then the solution was heated to make it clear. Followed by filtration, the hot filtrate was allowed to cool slowly for several hours. Then the yellow crystal formed was collected along with its mother liquor for X-ray crystallographic analysis. Yield: 55% (52 mg, 0.022 mmol).

Single-crystal X-ray diffraction

The X-ray intensity data for **1** were collected on a standard Siemens SMART CCD area detector system equipped with a normal-focus molybdenum-target X-ray tube (λ = 0.71073 Å) operated at 2.0 kW (50 kV, 40 mA) and a graphite monochromator at T = 293(2) K. The structures were solved by using direct methods and refined, employing full-matrix least squares on F^2 (Siemens, SHELXTL-97).[22] The X-ray intensity data for **3** and **4** were collected on a Rigaku MM-007 rotating anode diffractometer equipped with a Saturn CCD Area Detector System using monochromated Mo Kα (λ = 0.71070 Å) radiation at T = 113(2) K. Data collection and reduction were performed using the program Crystalclear.[23] A summary of crystal data and structure refinements is given in Table 1. For crystallographic data in CIF or other electronic format see DOI: 10.1039/b717884k.

To satisfy the charge balance, the C4AS in **1** should possess one protonated sulfonate group, which is acceptable given the pH of the reaction solution. Unfortunately, it was not possible to locate all hydrogen atoms from the Fourier difference map for this to be clarified.[24]

Table 1 Crystals structure data and details of structure refinements for **1**, **3** and **4**

Crystal data	1	3	4
CCDC deposit No.	666758	657145	657146
Empirical formula	$C_{55}H_{63}N_3O_{25}S_4$	$C_{96}H_{115}N_6O_{42.50}S_6$	$C_{96}H_{120}N_6O_{51}S_6$
Formula weight	1294.3	2225.3	2366.3
Crystal size/mm	0.30 × 0.26 × 0.20	0.16 × 0.14 × 0.12	0.32 × 0.16 × 0.14
Crystal system	Monoclinic	Triclinic	Triclinic
Space group	$P2_1/c$	$P\bar{1}$	$P\bar{1}$
a/Å	12.9696(16)	11.0638(11)	12.131(2)
b/Å	23.274(3)	12.9848(11)	12.741(2)
c/Å	20.884(3)	19.8264(8)	17.734(3)
α/°	90	73.838(15)	102.191(3)
β/°	103.405(2)	73.607(11)	103.227(4)
γ/°	90	87.276(18)	90.240(2)
Volume/Å^3	6132.3(13)	2623.0(4)	2604.1(8)
Z	4	1	1
D_{calc}/g cm^{-3}	1.402	1.409	1.509
$F(000)$	2712	1169	1242
μ(Mo Kα)/mm^{-1}	0.239	0.224	0.236
Temperature/K	294(2)	113(2)	113(2)
R_{int}	0.041	0.033	0.027
Range of h, k, l	–15/14, –27/27, –13/24	–13/13, –16/16, –24/24	–15/15, –16/16, –19/23
$\theta_{min/max}$/°	1.33/25.01	1.63/26.00	1.64/27.88
Reflections collected/uniqued	30840/10805	21257/10069/	24594/12178
Data/restraints/parameters	10805/234/980	10069/96/732	12178/93/870
Goodness of fit on F^2	1.046	1.071	1.071
Final R indices [$I > 2\sigma(I)$	$R_1 = 0.0719$	$R_1 = 0.0881$	$R_1 = 0.0559$
	$wR_2 = 0.2049$	$wR_2 = 0.2268$	$wR_2 = 0.1346$
R indices (all data)	$R_1 = 0.1223$	$R_1 = 0.1002$	$R_1 = 0.0740$
	$wR_2 = 0.2642$	$wR_2 = 0.2366$	$wR_2 = 0.1469$

Acknowledgements

This work was supported by 973 Program (2006CB932900), NNSFC (Nos. 90306009, 20673061 and 20703025) and the Science and Technology Innovation Foundation of Nankai University, which are gratefully acknowledged.

References

1 L. J. Barbour and J. L. Atwood, *Chem. Commun.*, 2001, 2020.
2 G. Arena, A. Casnati, L. Mirone, D. Sciotto and R. Ungaro, *Tetrahedron Lett.*, 1997, **38**, 1999; G. Arena, A. Casnati, A. Contino, G. G. Lombardo, D. Sciotto and R. Ungaro, *Chem.–Eur. J.*, 1999, **5**, 738; G. Arena, A. Casnati, A. Contino, F. G. Gulino, D. Sciotto and R. Ungaro, *J. Chem. Soc., Perkin Trans. 2*, 2000, 419; V. Ball, M. Winterhalter, F. Perret, G. Esposite and A. W. Coleman, *Chem. Commun.*, 2001, 2276; G. Arena, S. Gentile, F. G. Gulino, D. Sciotto and C. Sgarlata, *Tetrahedron Lett.*, 2004, **45**, 7091; J. P. Morel and N. Morel-Desrosiers, *Org. Biomol. Chem.*, 2006, **4**, 462.
3 A. W. Coleman, S. G. Bott, S. D. Morley, C. M. Means, K. D. Robinson, H.-M. Zhang and J. L. Atwood, *Angew. Chem., Int. Ed. Engl.*, 1988, **27**, 1361.
4 S. J. Dalgarno, J. L. Atwood and C. L. Raston, *Chem. Commun.*, 2006, 4567; S. J. Dalgarno and C. L. Raston, *Chem. Commun.*, 2002, 2216.
5 A. Drljaca, M. J. Hardie, J. A. Johnson, C. L. Raston and H. R. Webb, *Chem. Commun.*, 1999, 1135.
6 M. J. Hardie and C. L. Raston, *J. Chem. Soc., Dalton Trans.*, 2000, 2483; A. Drljaca, M. J. Hardie, C. L. Raston and L. Spiccia, *Chem.–Eur. J.*, 1999, **5**, 2295; A. Drljaca, M. J. Hardie and C. L. Raston, *J. Chem. Soc., Dalton Trans.*, 1999, 3639; A. Drljaca, M. J. Hardie, S. Airey and C. L. Raston, *Chem. Commun.*, 1999, 1137.
7 G. W. Orr, L. J. Barbour and J. L. Atwood, *Science*, 1999, **285**, 1049; J. L. Atwood, L. J. Barbour, S. J. Dalgarno, M. J. Hardie, C. L. Raston and H. R. Webb, *J. Am. Chem. Soc.*, 2004, **126**, 13170.
8 H. R. Webb, M. J. Hardie and C. L. Raston, *Chem.–Eur. J.*, 2001, **7**, 3616; S. J. Dalgarno and C. L. Raston, *Chem. Commun.*, 2002, 2216; S. J. Dalgarno, M. J. Hardie and C. L. Raston, *Cryst. Growth Des.*, 2004, **4**, 227.
9 J. L. Atwood, L. J. Barbour, S. J. Dalgarno, C. L. Raston and H. R. Webber, *J. Chem. Soc., Dalton Trans.*, 2002, 4351.
10 J. L. Atwood, L. J. Barbour, M. J. Hardie and C. L. Raston, *Coord. Chem. Rev.*, 2001, **222**, 3.
11 S. J. Dalgarno, M. J. Hardie, J. L. Atwood and C. L. Raston, *Inorg. Chem.*, 2004, **43**, 6351.
12 J. L. Atwood, S. J. Dalgarno, M. J. Hardie and C. L. Raston, *Chem. Commun.*, 2005, 337.
13 J. L. Atwood, S. J. Dalgarno, M. J. Hardie and C. L. Raston, *New J. Chem.*, 2004, **28**, 326.
14 S. J. Dalgarno, M. J. Hardie, M. Makha and C. L. Raston, *Chem.–Eur. J.*, 2003, **9**, 2834.
15 M. Makha, C. L. Raston, A. N. Sobolev and A. H. White, *Chem. Commun.*, 2005, 1962.
16 Y. Liu, Q. Li, D.-S. Guo and K. Chen, *Cryst. Growth Des.*, 2007, **7**, 1672.
17 Y. Liu, D.-S. Guo, H.-Y. Zhang, F. Ding, K. Chen and H.-B. Song, *Chem.–Eur. J.*, 2007, **13**, 466; M. Makha, C. L. Raston, A. N. Sobolev and A. H. White, *Chem. Commun.*, 2005, 1066; A. Drljaca, M. J. Hardie, J. A. Johnson, C. L. Raston and H. R. Webb, *Chem. Commun.*, 1999, 1135; M. Selkti, A. W. Coleman, I. Nicolis, N. Douteau-Guével, F. Villain, A. Tomas and C. de Rango, *Chem. Commun.*, 2000, 161; M. J. Hardie, J. A. Johnson, C. L. Raston and H. R. Webb, *Chem. Commun.*, 2000, 849; S. J. Dalgarno, M. J. Hardie and C. L. Raston, *Cryst. Growth Des.*, 2004, **4**, 227.
18 Y. Liu, K. Chen, D.-S. Guo, Q. Li and H.-B. Song, *Cryst. Growth Des.*, 2007, **7**, 2601.
19 J. R. Platt, *J. Chem. Phys.*, 1949, **17**, 484; K. Harata and H. Uedaira, *Bull. Chem. Soc. Jpn.*, 1975, **48**, 375.
20 F. Ugozzoli and G. D. Andreetti, *J. Inclusion Phenom. Mol. Recognit. Chem.*, 1992, **13**, 337.
21 G. Arena, A. Contino, G. G. Lombardo and D. Sciotto, *Thermochim. Acta*, 1995, **264**, 1(*a*) S. Shinkai, S. Mori, H. Koreishi, T. Tsubaki and O. Manabe, *J. Am. Chem. Soc.*, 1986, **108**, 2409.
22 SHELX97: G. M. Sheldrick, University of Göttingen, Germany, 1997.
23 *CrystalStructure 3.7.0 and Crystalclear 1.36: Crystal Structure Analysis Package*; Rigaku and Rigaku/MSC (2000–2005): The Woodlands, TX.
24 S. J. Dalgarno, J. L. Atwood and C. L. Raston, *Cryst. Growth Des.*, 2006, **6**, 174.

